Effect of Surface Morphology on Dimerization of *tert*-Butyl Mercaptan on the Surface of Amorphous Aluminosilicate Impregnated with Mn and Cu

Jeong Eun Kweon, Hyunha Joo, and Dong Gon Park*

*Department of Chemistry, Sookmyung Women's University, Seoul 140-742, Korea. *E-mail: dgpark@sookmyung.ac.kr*
Received August 9, 2005

A powder of destructive adsorbent was prepared by impregnating Mn and Cu on the surface of amorphous aluminosilicate. It catalytically dimerized *tert*-butyl mercaptan into di-*tert*-butyl disulfide on its surface. Turnover of the dimerization was strongly dependent on the surface morphology of the adsorbent, which could be altered by modification of aluminosilicate support. During the process of impregnation, which involved heat-treatment at 500 °C, the shape of the pore was preserved, though large fraction of micropores were eliminated. The reactive sites on the surface were poisoned as dimerization products strongly adhered on them. Therefore, high surface area was not always desirable. When the surface was heavily populated with "ink-bottled" pores with a narrow entrance in uniform size, heavy poisoning of the reactive sites turned the destructive adsorbents almost useless.

Key Words : Aluminosilicate, *tert*-Butyl mercaptan, Dimerization, Porosimetry

Introduction

As the living standard improves, there has been much concern on comfortable living environment. As living space tends to adopt more closed setting than in the past, much demand and research effort has been created to put "malodor" under control.[1-3] Common sources of the bad smell around living space are foods. The smell from the foods gets especially unpleasant when they become over-fermented or rotten. In a few far-eastern countries, such as Korea and Japan, variety of fermented foods are daily consumed, which contain both fish or garlic. When over-fermented or rotten, these foods tend to produce various malodorant volatile compounds. Most of these malodorant compounds fall into two categories, mercaptan and amine derivatives.[4,5]

Even very small amount of mercantan compounds gives very strong unpleasant sensation to human olfactory nerves. We deal with those malodorant compounds everyday, without knowing they consist of mercaptan compounds. As an example, methyl mercaptan (CH_3SH) is a major gas compound generated from over-fermented Kimchi products. It is very pervasive compound that it ruins plastic containers, woven products, even tastes of all other nearby foods including water and ice. *tert*-Butyl mercaptan, TBM (C_4H_9SH), also has very strong unpleasant stench. As a safety measure, TBM has intentionally been added into a flammable gas, such as liquefied natural or propane gasses (LNG, or LPG).[6] Mixing process for TBM into liquefied gases often accompanies very small amount of a leak, which triggers a false alarm.

The most common measure to control malodorant volatile compounds is to use adsorbents, porous solids with high surface area, such as activated carbons or zeolites. They utilize simple physisorption as a means to get rid of the malodorant volatile compounds. Commercial deodorizing products in the market nowadays are mostly these adsorbents. Because the malodorants are removed only by physisorption, the lifetime of this kind is very limited. Malodorants can also be passified via oxidation by ozone.[1] But, a device for ozone generation is rather expensive, and it keeps consuming electric energy during the use. Moreover, mercaptans are resistant to oxidizing agents.

As an alternative way to get rid of stench from alkyl-mercaptan compounds without energy consumption, we previously suggested the use of destructive adsorbents, which are porous silica impregnated with transition metals, active to the catalytic dimerization of mercaptans.[7] On the surface of the destructive adsorbents, alkyl mercaptan was dimerized into dialkyl disulfide, and its malodor was passified. It was shown that oxygen in the atmosphere is closely involved in the dimerization reaction, possibly through scrambling with the lattice oxygen on the surface of the oxides.[8] Even though reaction mechanism is partly understood, influence by other factors, such as composition of the adsorbents, defects on the surface, porosity, and especially the surface morphology of the adsorbents, still remain unknown. In order to verify such influences, one should first get an appropriate means to prepare comparison samples. We report preparation of two different comparison samples of the destructive adsorbents by modifying surface morphology of amorphous aluminosilicate supports through manipulation of precipitation process.

Experimental Section

Aqueous solution of silicate was prepared by dissolving 12.2 g of Na_2SiO_3 (reagent grade, Junsei Chemical) in 12 mL distilled water. In a separate container, aqueous solution of aluminate was prepared by dissolving 8.2 g of $NaAlO_2$ (reagent grade, Junsei Chemical) in 60 mL distilled water. Mole ratio of Si to Al was roughly one to one. The aluminate

solution was dropwise added into the silicate solution, which turned the mixture into a thick colloidal solution. The coagulated colloidal solution was peptized into aluminosilicate sol by adding 60 mL of 6 N HCl solution during several hours. Then, coprecipitation into aluminosilicate hydrogel was carried out by dropwise addition of 6 N NaOH into the aluminosilicate sol. During all the mixing processes, the mixture was vigorously agitated using a mechanical stirrer. The addition of the NaOH solution was terminated when basicity of the solution reached pH=7, or pH=11. The precipitate was collected by filtration. After salt was removed by thorough washing, the precipitate was dried overnight in an oven at 120 °C, and was used as a support for the destructive adsorbent. For descriptive convenience, the amorphous aluminosilicate powders obtained at pH=7 and pH=11 will be designated as $Al_2Si_2O_7$ (pH 7) and $Al_2Si_2O_7$ (pH 11), respectively.

About 2 g of the aluminosilicate support was weighed and dispersed in 100 mL distilled water. In a separate container, $Mn(NO_3)_2{\cdot}4H_2O$ and $Cu(NO_3)_2{\cdot}3H_2O$ (both reagent grade, Deoksan Chemical) were dissolved in a minimal amount of water, and added over the aluminosilicate. The amounts of the metal constituents were adjusted to 8 and 4% to the weight of the aluminosilicate support, for Mn and Cu, respectively. In a water bath at around 80 °C, the mixture was turned into a wet paste by slowly removing water from it. After overnight drying in an oven at 120 °C, the dark brown solid was further ground into a fine powder. By heating at 500 °C for 12 h under nitrogen atmosphere, the brown powder was turned into the destructive adsorbent, aluminosilicate impregnated with Mn and Cu, which will be designated as '[Mn/Cu]$Al_2Si_2O_7$'.

Nitrogen isotherms were measured by Micromerities ASAP 2400. Surface area was calculated by BET method.[9] Pore size distribution was calculated by BJH method from the desorption curve of the nitrogen isotherm.[10] Information on micropores in the powder sample was obtained by t-plot derived from the adsorption curve of the isotherm.[9] FTIR spectra were in-situ measured by Nicolet Impact 400 spectrophotometer from head-gas over 0.1 g of [Mn/Cu]$Al_2Si_2O_7$ powder in a cylindrical gas cell (50 mL inner volume). TBM was injected as a pulse into the cell over the powder, so that the initial concentration of TBM was 5 ppt. Immediately after injection, FTIR spectrum was taken every 3 min. Eight to ten measurements were made for each pulse. The gas product was also characterized by gas-chromatograph/mass-spectrometry (GC-MS), using Finnigan Automass 300. In a homemade reactor vessel (100 mL inner volume), liquid mercaptan was in-situ evaporated over 0.1 g [Mn/Cu]$Al_2Si_2O_7$ powder, and GC/MS measurements were carried out on aliquots of the head-gas over the time. The initial concentration of TBM in the reactor was adjusted to 100 ppt, which would render the amount of TBM to be 40-fold larger than in the previous FT-IR measurements.

Results and Discussion

Mechanism of particle growth in a silicate solution is well understood.[11] Solid particles in the solution tend to form an interwoven network structure of silica hydrogel in the range of pH 7 to 10, when salt is present in the solution of silicic acid. Without salt, inter-condensation of the particles is suppressed, and they tend to grow into large colloidal particles via Ostwald ripening. In higher pH, ripening of the particles is also enhanced. Unlike in a single component system, the mechanism of particle growth is not much studied for multi-component system, where hydroxides of more than two metals are involved. But, it is suggested that it

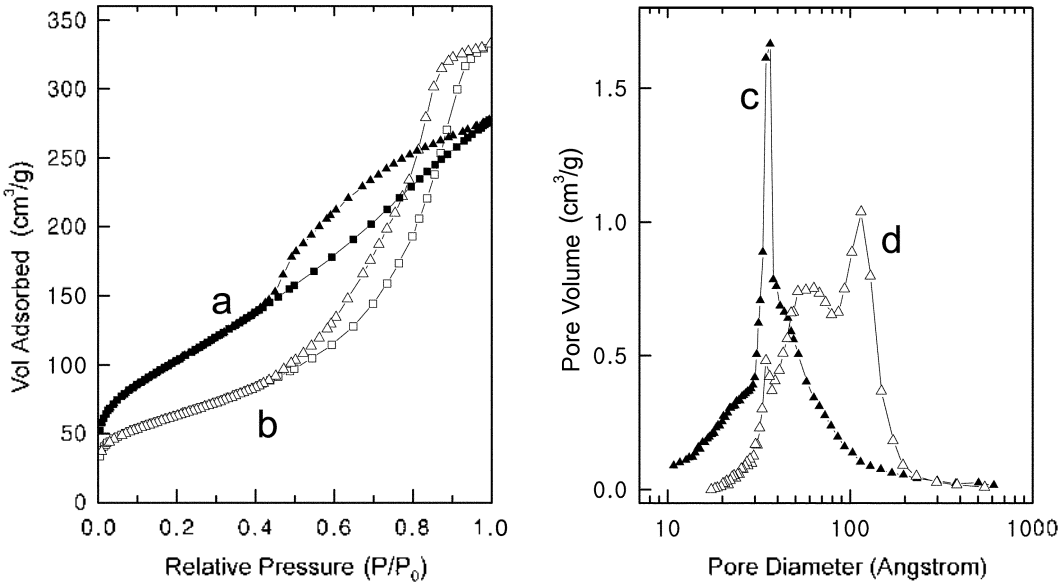

Figure 1. Isotherms of nitrogen adsorption-desorption measured for amorphous aluminosilicate supports, (a) on the surface of $Al_2Si_2O_7$ (pH 7), (b), and on the surface of $Al_2Si_2O_7$ (pH 11). Pore size distributions, (c) for $Al_2Si_2O_7$ (pH 7), and (d) for $Al_2Si_2O_7$ (pH 11). The distribution was calculated by BJH method from the desorption curve of the corresponding isotherm.

would be similar to the one for the silicic acid.

When aqueous solutions of silicate and aluminate were mixed together, they immediately solidified into a mass that further manipulation was not possible. Slow dropwise addition with a vigorous agitation, and addition of aluminate over silicate solution, not the other way, was crucial to get a colloidal solution of aluminosilicate. A portion of the solution was set aside in order to collect aluminosilicate particles in the solution by filtration. BET surface area of the aluminosilicate particles at this stage was mere 7.8 m^2/g, and was too small for the use as a support.

Modification of the colloidal aluminosilicate was carried out via peptization followed by condensation. Peptization broke down the colloidal particles into much smaller ones. As dissolution of the particles proceeded, the white non-transparent solution turned into a clear one with some haziness, which indicated the size of the particles was below 100 nm. The small particles were reassembled into bigger ones by condensation among them. The particle growth via condensation was initiated by addition of NaOH into the solution, which turned the solution turbid. After the treatment, amorphous aluminosilicate was obtained in morphology very different from the original colloidal solids.

The BET surface area of the amorphous powders of aluminosilicates obtained after the modification increased more than 30-fold (from 7.8 to 370, and 230 m^2/g in Table 1). In lower pH, average pore diameter gets smaller, and BET surface area gets larger. This observation indicates the surface morphology of the aluominosilicate was modified by pH of the solution during condensation among particles. Figure 1a and 1b shows the isotherms of nitrogen adsorption-desorption on those two different powder samples. They both exhibit hysteresis, which provides information on the structure of the pore. Type H2 hysteresis in Figure 1a indicates $Al_2Si_2O_7$ (pH 7) has pores with a uniform sized small entrance, like in parallel slits or so called "ink-bottled" pores.[9,10] The size of the entrance has fairly narrow distribution around 35 Å, as assessed by the pore size distribution curve in Figure 1c. On the contrary, the isotherm for $Al_2Si_2O_7$ (pH 11) has type H1 hysteresis, in Figure 1b, indicating it has cylindrical pores.[10] The size of the cylindrical pores is widely distributed from around 35 to 150 Å as seen in Figure 1d.

They also contain micropores, by seeing that the infliction of the isotherm is raised at lower end of the relative pressure. Microporous surface areas were calculated from the slopes

Table 1. Pore characteristics for the supports and destructive adsorbents

Sample	S_t	ΔS_t	d_{aver}	S_{micro}	ΔS_{micro}	$S_{meso-macro}$
Before modification	7.8	–	–	–	–	–
$Al_2Si_2O_7$ (pH 7)	370.2	–	46.4	324.5	–	45.7
$Al_2Si_2O_7$ (pH 11)	229.6	–	89.6	184.0	–	45.6
[Mn/Cu]$Al_2Si_2O_7$ (pH 7)	189.1	181.1	53.0	151.1	173.4	38.0
[Mn/Cu]$Al_2Si_2O_7$ (pH 11)	129.2	100.4	108.7	87.0	97.0	42.2

S_t: total surface area BET surface area. d_{aver}: average pore diameter. $S_{meso-macro}$: surface area by mesopores and macropores, calculated from t-plot. S_{micro}: surface area by micropores = $S_t - S_{meso+micro}$. Δ: change after impregnation and heat-treatment.

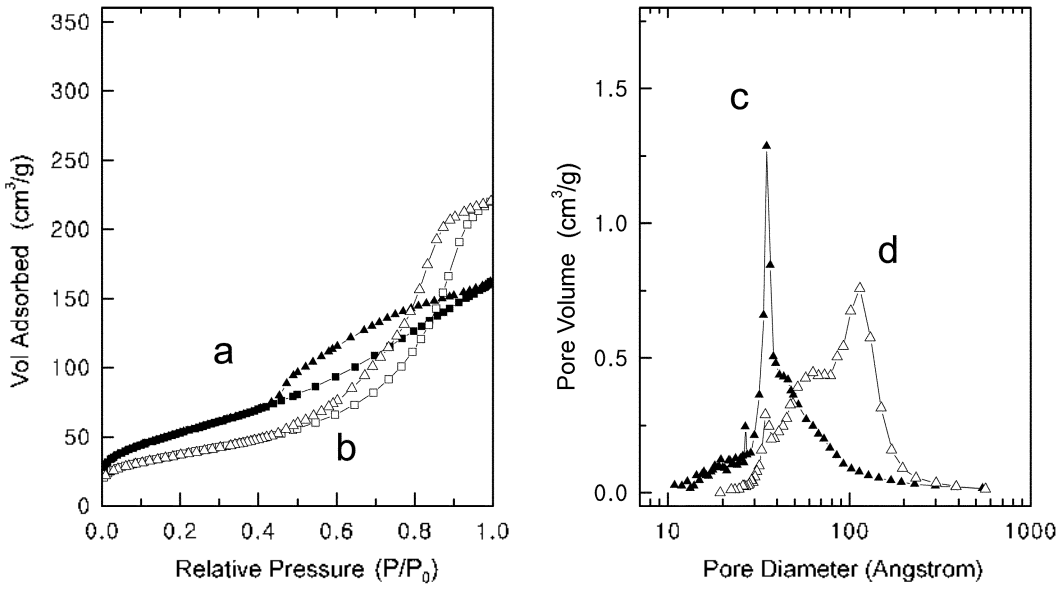

Figure 2. Isotherms of nitrogen adsorption-desorption measured for destructive adsorbents, (a) on the surface of [Mn/Cu]$Al_2Si_2O_7$ (pH 7), (b), and on the surface of [Mn/Cu]$Al_2Si_2O_7$ (pH 11). Pore size distributions, (c) for [Mn/Cu]$Al_2Si_2O_7$ (pH 7), and (d) for [Mn/Cu]$Al_2Si_2O_7$ (pH 11). The distribution was calculated by BJH method from the desorption curve of the corresponding isotherm.

of the t-plots derived from the isotherms,[9] and are provided in Table 1. In $Al_2Si_2O_7$ (pH 7), micropores contribute more to the total surface area than in $Al_2Si_2O_7$ (pH 11). This observation suggests the particle size was smaller at lower pH, which conforms to the prediction based on the study on the silica sol. A study on the generation of silica particles from silicic acid suggests that the rate of condensation among particles competes with the speed of particle growth by Ostwald ripening, when the solution contains salt which can alleviate repulsion among negatively charged particles.[11] Because aluminosilicate solution contained plenty of salt, which came from HCl and NaOH, highly branched interwoven network structure should result when pH was below 10. As it gets more basic, the size of the particle shall increase, because particle growth will be enhanced, and network formation will be suppressed.

Once obtaining a leverage to control the pore morphology of the support, our next concern was whether it would be sustained through out the subsequent impregnation and heat-treatment at 500 °C. It was shown, in our previous studies, that the heat-treatment during impregnation largely altered the shape of the pore, in silica aerogel[7] and magnesia aerogel.[12] The isotherms of nitrogen adsorption-desorption were shown in Figure 2 for those desteructive adsorbents, [Mn/Cu]$Al_2Si_2O_7$ (pH 7) and [Mn/Cu]$Al_2Si_2O_7$ (pH 11). BET surface area, average pore diameter, and surface area from micropores are provided in Table 1. Considering that the shape of the hysteresis was preserved (compare figure 1a-b with 2a-b), the pore morphology of the aluminosilicate support was not much altered even after impregnation with nitrates of Mn and Cu, followed by heating at 500 °C.

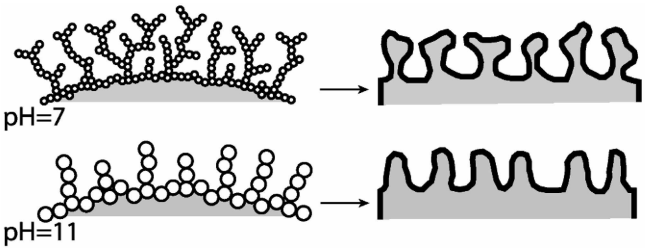

Figure 3. Hypothetical cross-sections of the destructive adsorbents constructed on the basis of the observations by porosimetry. The surface of the samples prepared at pH=7 has mesopores with narrower entrances, and has higher population of micropores, than those obtained at pH=11.

Even though it did not change the shape of the pore, heat-treatment caused a significant decrease in BET surface area (see table 1). The extent of the decrease was especially large (ΔS_t = 181 m^2/g) in [Mn/Cu]$Al_2Si_2O_7$ (pH 7). It is interesting to note that the extent of the decrease accompanied by impregnation is nearly identical for ΔS_t and ΔS_{micro}. It suggests that the loss of the surface area was mostly caused by elimination of the micropores. The value of $S_{meso+macro}$ did not change much after the heat-treatment. This conforms to the observation that size distribution curves did not change much over the mesoporous range (compare figure 1c-b with figure 2c-d). Based on these observations, hypothetical cross-sectional view of [Mn/Cu]$Al_2Si_2O_7$ (pH 7) was compared to that of [Mn/Cu]$Al_2Si_2O_7$ (pH 11) in Figure 3.

In previous report, it was shown that *tert*-butyl mercaptan (TBM) dimerizes into di-*tert*-butyl disulfide (DBDS) over the surface of silica impregnated with Mn and Cu, through

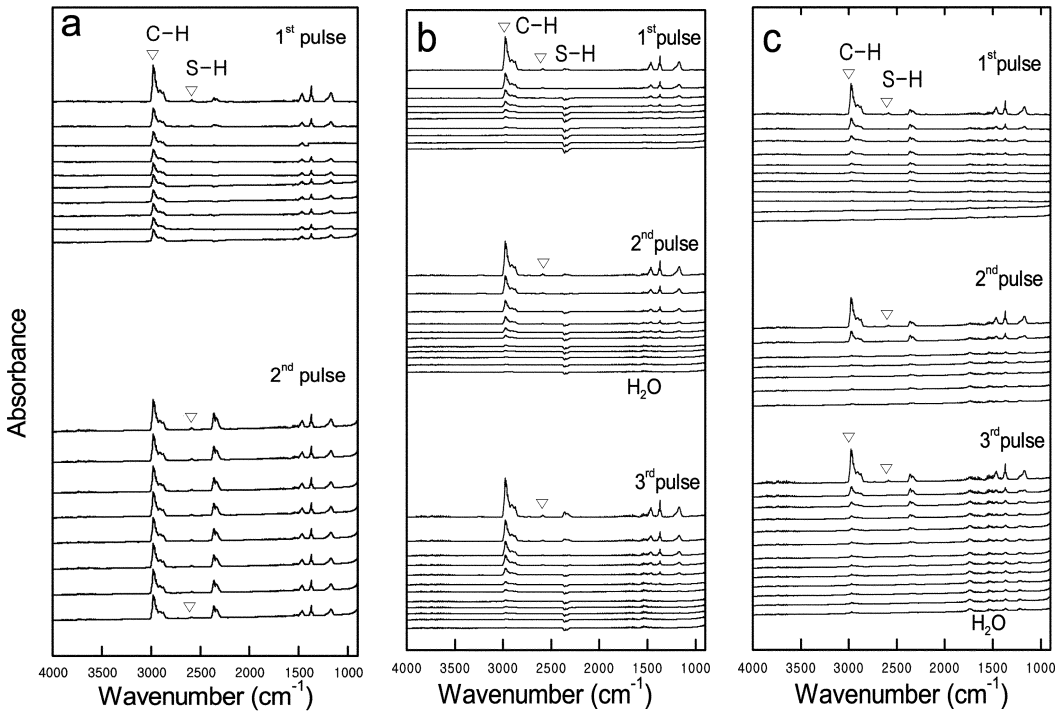

Figure 4. FTIR spectra taken for the consecutive pulses of TBM, (a) over the blank support, aluminosilicate without [Mn/Cu] impregnated, (b) over the surface of [Mn/Cu]$Al_2Si_2O_7$ (pH 7), and (c) over the surface of [Mn/Cu]$Al_2Si_2O_7$ (pH 11). The lapse between consecutive spectra was 3 min. Each cluster of the spectra represents measurements on one pulse of TBM.

the following reaction.[8]

$$2C_4H_9SH + 1/2O_2 \rightarrow C_4H_9SSC_4H_9 + H_2O \quad \Delta H < 0$$

Without oxygen in the overhead gas, the reaction would not proceed. FT-IR spectra are very similar for both TBM and DBDS, except a few characteristic peaks by TBM. In discerning the reactant from the product, the best guidance is provided by the S-H vibration of TBM at 2600 cm $^{-1}$. The C-H vibration is also slightly shifted to 2990 cm $^{-1}$ in TBM. In order to verify the catalytic role of the impregnated transition metals over the surface of aluminosilicate, a blank support was prepared by heat-treating $Al_2Si_2O_7$ (pH 11) at 500 °C without being impregnated. Over this blank support, a pulse of TMB was injected and in-situ monitored by FT-IR, as shown in Figure 4a. Dimerization reaction of TBM was not occurring over the surface of aluminosilicate, when it was not impregnated. Characteristic peaks of TBM at 2600 and 2990 cm $^{-1}$ are persistent over the time (see second pulse in figure 4a).

On the contrary, when TBM was injected over [Mn/Cu]$Al_2Si_2O_7$ (pH 11), in Figure 4c, those two peaks started decreasing immediately. They disappeared in 10-15 min, which indicates TBM was readily dimerized into DBDS over the surface of aluminosilicate impregnated with Mn and Cu. Steady growth of water peaks around 1700 and 3700 cm $^{-1}$ is also apparent, as the number of pulses adds up. Same observation was also made in Figure 4b for [Mn/Cu]$Al_2Si_2O_7$ (pH 7). TBM peaks disappear in 10-15 min, and water peaks adds up with consecutive injections of TBM pulses. Therefore, both [Mn/Cu]$Al_2Si_2O_7$ (pH 7) and [Mn/Cu]$Al_2Si_2O_7$ (pH 11) showed catalytic reactivity toward dimerization reaction of TBM, at least for a small quantity of it.

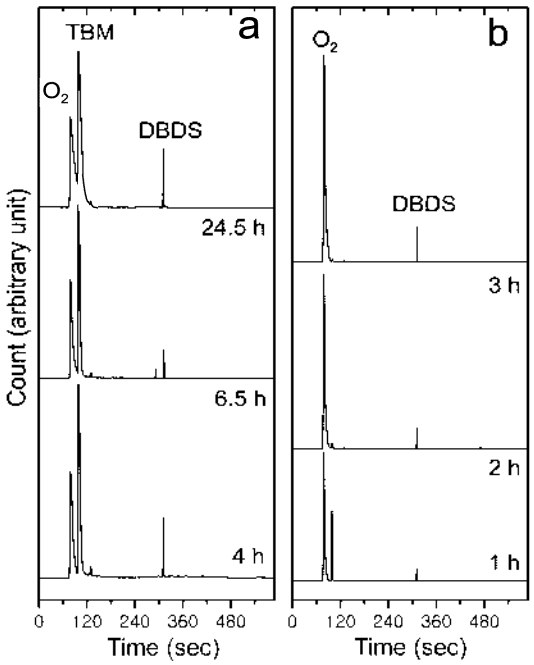

Figure 5. Gas chromatographs of the overhead gas obtained after designated time. The overhead gas was taken, (a) from [Mn/Cu]-$Al_2Si_2O_7$ (pH 7), and (b) from [Mn/Cu]$Al_2Si_2O_7$ (pH 11).

Dimerization reaction on larger quantity of TBM over the surface of [Mn/Cu]$Al_2Si_2O_7$ (pH 7) and [Mn/Cu]$Al_2Si_2O_7$ (pH 11) was monitored by GC/MS, shown in Figure 5. The reaction of a larger quantity (40-fold) of TBM exhibits quite different outcome from the one seen by FT-IR above. The reaction over [Mn/Cu]$Al_2Si_2O_7$ (pH 7) was very slow that major portion of TBM was still registered as a large peak, in Figure 5a, even after a day. Even though the BET surface area was larger (189.1 vs 129.2 m^2/g) than [Mn/Cu]$Al_2Si_2O_7$ (pH 11), [Mn/Cu]$Al_2Si_2O_7$ (pH 7) was not efficient in catalyzing dimerization at all. On the contrary, dimerization of TBM by [Mn/Cu]$Al_2Si_2O_7$ (pH 11) was almost complete in two hours (figure 5b). After three hours, a sensual test over an open vessel registered no stench from TBM at all.

Because vapor pressure of DBDS (2.45 kPa at 25 °C) is much lower than that of TBM (24.2 kPa at 25 °C), DBDS would preferably condense into the pores once generated on the surface. In a previous GC-study on aerosil[8] impregnated with Mn and Cu,[8] an elemental analysis showed that considerable amount of DBDS was staying on the surface. As surface was saturated by physisorbed DBDS, dimerization of TBM was largely suppressed, presumably because reactive sites could not be reached by incoming TBM.

The strikingly different outcome of the GC-MS measurements above suggests that the morphology of a surface is a major reason to influence adsorption and desorption processes on the surface of solids. The difference in the pore shapes in Figure 4 provides a clue to this observation. The volume of DBDS molecule is about twice larger than TBM. Therefore, TBM easily enters into so called "ink-bottled" pores on the surface of [Mn/Cu]$Al_2Si_2O_7$ (pH 7). But as TBM dimerizes into much larger DBDS in the "bottle", out bound flux of the product gas is largely blocked. Unless DBDS is flushed out of the "bottle", the equilibrium of the adsorption and desorption of DBDS would shift toward adsorption inside these "bottled" pores. Thereby, access to reactive sites by incoming TBM is namely denied in [Mn/Cu]$Al_2Si_2O_7$ (pH 7). On the contrary, cylindrical shape of the pores in [Mn/Cu]$Al_2Si_2O_7$ (pH 11) with a range of different sizes, apparently gave better chance to release DBDS, thereby, readily exposing reactive sites to incoming TBM. Moreover, the surface of [Mn/Cu]$Al_2Si_2O_7$ (pH 7) contains more micropores, as can be seen in Table 1, than in [Mn/Cu]$Al_2Si_2O_7$ (pH 11). Therefore, DBDS would adhere more adamantly on the surface of [Mn/Cu]$Al_2Si_2O_7$ (pH 7), blocking the reactive sites.

Similar observation was made in previous study on silica aerosil[8] impregnated with Mn and Cu, that turnover kept decreasing as large amount of TBM was passed over the destructive adsorbent. These observations indicate that active sites are poisoned by product of the very reaction they catalized. Even though the active sites can be revived by heating, via reverse reaction below, such necessity will tarnish the commercial value of the destructive adsorbent.

$$C_4H_9SSC_4H_9 + H_2O \rightarrow 2C_4H_9SH + 1/2O_2 \quad \Delta H > 0$$

Therefore, it would be better to adjust surface morphology

so that the adsorption of reactant and release of product would be well balanced.

Conclusions

Amorphous aluminosilicates in large surface area were prepared by precipitation of aluminosilicate sol. By adjusting pH during the precipitation, aluminosilicates in different morphologies could be obtained. The aluminosilicate prepared at pH=7 contained so called "ink-bottled" pores, while the one obtained at pH=11 had cylindrical ones. For both samples, major fraction of total surface area was from micropores.

These aluminosilictes in the different surface morphologies were used as supports for the destructive adsorbents, whose surface was impregnated with Mn and Cu. During the process of the impregnation and subsequent heat-treatment, the shape of the pore was preserved, while a large fraction of micropores was eliminated, which accompanied the loss of BET surface area.

When impregnated with Mn and Cu, the surface of amorphous aluminosilicates turned highly reactive toward dimerization of TBM, catalytically turning it into DBDS. The rate of dimerization was strongly dependent on the surface morphology. When the surface had high population of "ink-bottled" mesopores, the catalytic reactivity of the surface was largely spoiled, if once dimerization got started. It is suggested that access by incoming TBM over the reactive sites were blocked as DBDS got trapped in the pores and adhered on the reactive sites. Apparently, poisoning was not that severe when the surface had cylindrically shaped mesopores in a wide range of the size.

References

1. Yoshimoto, M.; Nakatsuji, T.; Yoshida, K. *Jpn. Kokai Tokkyo Koho JP* 04,277,014, 1992.
2. Okuda, Y. *Jpn. Kokai Tokkyo Koho JP* 06,122,519, 1994.
3. Becker, O.; Kolz, S.; Hager, H. *Eur. Pat. Appl. EP* 633065, 1995.
4. Cha, Y. S.; Cadwallader, K. R. *J. Food Sci.* **1995**, *60*(1), 19.
5. Martin-Lagos, R. A.; Olea Serrano, M. F.; Ruiz Lopez, M. D. *Food Chem.* **1995**, *53*, 91.
6. *Odorization II*; Wilson, G. G., Attari, A. A., Eds.; Institute of Gas Technology: Chicago, Illinois, USA, 1998.
7. Park, S. H.; Park, D. G; Kweon, H. J.; Nam, S. S.; Kim, S. B.; Lee, Y. B.; Choe, K. H. *Bull. Korean Chem. Soc.* **1999**, *20*(6), 639.
8. Park, D. G.; Park, S. H.; Lee, S. J. *Bull. Korean Chem. Soc.* **2000**, *21*(7), 715.
9. Lowell, S.; Shields, J. E. *Powder Surface Area and Porosity*; 3rd Ed.; Chapman & Hall: London, UK, 1991; p 11.
10. Gregg, S. J.; Sing, K. S. W. *Adsorption, Surface Area and Porosity*; 2nd Ed.; Academic press: Londodn, UK, 1982; p 111.
11. Brinker, C. J.; Scherer, G. W. *Sol-Gel Science: The Physics and Chemistry of Sol-Gel Processing*; Academic press: San Diego, USA, 1990; pp 97-107.
12. Kim, H. J.; Kang, J.; Park, D. G.; Kweon, H. J.; Klabunde, K. J. *Bull. Korean Chem. Soc.* **1997**, *18*(8), 831.